Journal of Clinical & Experimental Cardiology

Mihai et al. J Clinic Experiment Cardiol 2011, 2:9
DOI: 10.4172/2155-9880.1000152

Research Article Open Access

Design and Rationale for the Study of Changes in Iron and Atherosclerosis Risk in Perimenopause

Georgeta Mihai, Xin He, Xiaolan Zhang, Beth McCarthy, Tam Tran, Michael Pennell, Jessica Blank, Orlando P. Simonetti, Rebecca D. Jackson and Subha V. Raman*

Ohio State University, Davis Heart and Lung Research Institute, 473 W. 12th Ave, Suite 200, Columbus, OH 43210, USA

Abstract

This study seeks to investigate changes in iron homeostasis and carotid arteries in women at risk of atherosclerosis, addressing a relatively unexplored hypothesis explaining why women have a 5-10 year lag in initial atherosclerotic events. Recent evidence points to hepcidin, the key regulator of macrophage iron uptake and release, as a potential mediator of risk. Furthermore, iron catalyzes the generation of free radicals that oxidize cholesterol stimulating atheroma formation. Magnetic resonance imaging (MRI) is ideally suited to study iron because of iron's local effects on magnetic susceptibility that can be quantified using a relaxation parameter called T2* ('T2-star'), as well as the ability to noninvasively characterize and quantify atherosclerotic plaque with MRI. This work outlines the rationale and study design to provide critical evidence related to the iron hypothesis, such that novel diagnostics and therapeutics to attenuate risk may be derived from a better understanding of iron's role in atherosclerosis.

Keywords: Atherosclerosis risk; Carotid artery; Magnetic resonance imaging; Iron; Women

Introduction

While the prevalence of atherosclerosis is similar in women and men, women enjoy a 5-10 year lag in onset of cardiovascular events compared to men [1]. After menopause, a state associated with marked reduction in ovarian sex steroid production, the relative risk of events such as heart attack and stroke caused by atherosclerotic plaque rises up to threefold regardless of age range [1]. This has prompted numerous investigations of hormone therapy (HT) to lower cardiovascular risk to premenopausal levels. However, initiating HT in large, randomized trials has not realized a cardiovascular benefit [2-4].

Another change that occurs following menopause that may contribute to atherosclerosis risk is cessation of monthly iron loss [5]. The remarkable *lack* of atherosclerosis in patients with iron overloaded states like hereditary hemochromatosis (HH) [6] has been used to argue against the 'iron hypothesis'. Recent advances in understanding iron homeostasis have identified an important hepatically-synthesized protein called hepcidin—a crucial regulator of macrophage iron uptake; its near absence in HH may explain these patients' relative protection from atherosclerosis. Together, increased available iron and hepcidin may yield redox-active iron able to oxidize lipid and fuel plaque progression; thus, more informed studies of iron and perimenopausal atherosclerosis risk that address both are warranted.

Iron in tissues affects local magnetic properties that can be quantified using the magnetic resonance imaging (MRI) parameter T2*, which decreases with increased tissue iron content. We sought to design a study testing the hypothesis that changes in iron homeostasis fuel the development of atherosclerosis, and that increased vascular iron content in women explains the postmenopausal woman's loss of relative protection against atherosclerotic events.

Methods and Trial Endpoints

Study objectives

The primary objectives of the present study are to 1) measure changes in arterial wall iron content in women entering menopause and 2) identify changes in the iron uptake signal hepcidin through perimenopause. The hypotheses driving this longitudinal study in a cohort of women entering menopause are the following: arterial wall iron increases in the transition from perimenopausal to postmenopausal status, carotid wall volume and dysfunction increases with increased arterial wall iron, and the macrophage iron uptake signal hepcidin increases after menopause in women at high risk of developing atherosclerosis.

Study design

This is an observational, prospective single-center cohort study approved by the Ohio State University Institutional Review Board, and all participants provide written, informed consent to participate.

Study population

Perimenopausal women, defined as women age 40 years or older with at least 1 but no more than 6 menstrual cycles in the 12 months preceding enrollment, with two or more of the following cardiovascular disease CVD risk factors are eligible: total cholesterol ≥ 240 mg/dL, diastolic blood pressure ≥90 mmHg, systolic blood pressure ≥140 mmHg, current smoker, or history of diabetes. In addition, 15 perimenopausal women with zero or one CVD risk factors are enrolled as controls. To avoid confounding effects on iron homeostasis, patients with a history of renal dysfunction (GFR ≤40 ml/min/m^2) or those unwilling to donate blood during the study will be excluded from enrollment. Excluded will be subjects with clinically-apparent atherosclerotic heart disease or peripheral arterial disease defined

***Corresponding author:** Subha V. Raman, MD, Professor, Ohio State University, Davis Heart and Lung Research Institute, 473 W. 12th Ave, Suite 200, Columbus, OH 43210, USA, Tel: 614 293-8963; Fax: 614 293-5614; E-mail: raman.1@osu.edu

Received September 07, 2011; **Accepted** October 03, 2011; **Published** October 08, 2011

Citation: Mihai G, He X, Zhang X, McCarthy B, Tran T, et al. (2011) Design and Rationale for the Study of Changes in Iron and Atherosclerosis Risk in Perimenopause. J Clinic Experiment Cardiol 2:152. doi:10.4172/2155-9880.1000152

as prior acute coronary syndrome, exertional angina or equivalent, prior coronary intervention or bypass surgery, claudication or prior peripheral vascular intervention will be excluded. Enrollment criteria are summarized in Table 1.

Measurements

Recruited eligible subjects will undergo baseline, one year and two years follow-up laboratory evaluations that include clinical assessment (e.g. body mass index, blood pressure and waist/hip circumference ratio), serologies and noncontrast MRI. Blood pressure is measured in the right or left arm while the patient is resting on the scanner table post-MRI. In addition to recording medications, intake of supplemental iron or multivitamin containing iron will be quantified in mg/month derived from a standardized food frequency questionnaire [7] completed at the second MRI visit. Follow-up phone interviews at 6-month intervals will document interval occurrence of atherosclerotic endpoints defined as any of the following: coronary heart disease events (coronary death, myocardial infarction, and angina); cerebrovascular events (including stroke and transient ischemic attack); peripheral artery disease; or heart failure due to ischemic heart disease. Any reported events will be further documented by review of the medical records by a blinded physician adjudicator.

Serologies including creatinine, lipid levels, iron, total iron-binding capacity, ferritin and high-sensitivity C-reactive protein will be measured at each MRI visit. Bioavailable estradiol will be measured using estradiol RIA (Esoterix, Inc.) and sex hormone binding globulin assays [8] at baseline, 1-year follow-up and 2-year follow-up. Plasma hepcidin is measured at each MRI visit using hepcidin-25 EIA (Bachem Americas, Inc.).

MRI

All subjects are imaged on a 3 Tesla whole body scanner (MAGNETOM Verio, Siemens Healthcare; Erlangen, Germany) with maximum gradient amplitude of 45mT/m and a slew rate of 200 mT/m/ms. The system's integrated body coil will be used for radiofrequency signal transmission. Signal reception will be assured by a flexible 6-element phase array body coil in combination with the table embedded spine coil for liver imaging and by a custom built 8-element (4 left and 4 right) carotid coil for carotid imaging (Massachussetts General Hospital). All subjects undergo the same imaging protocol that includes the elements outlined in Table 2.

Perimenopausal women
Inclusion criteria
Age ≥40 years
Female gender
Between 1 and 6 menstrual cycles in the last 12 months
GFR >40 mL/min/1.73 m^2
Hematocrit ≥ 35%
Willing to not donate blood during study
2 or more major risk factors[1] (study population) or 0 or 1 risk factors (controls)
Exclusion criteria
Inability/unwillingness to provide informed consent
Contraindication to MRI[2]
Known abnormality of iron metabolism[3]
Bleeding disorder or bleeding event in the past 6 months
Known atherosclerotic heart or peripheral vascular disease
Pregnancy
Use of hormone therapy
Active infection[4]

NOTES: 1-risk factors include hypertension, diabetes, smoking, and hyperlipidemia. 2-presence of ferromagnetic foreign body, aneurysm clip, any MR-incompatible implant, inability to fit in MRI scanner; 3-examples include hereditary hemochromatosis, iron deficiency, paroxysmal nocturnal hemoglobinuria, hemosiderosis for any reason, atransferrinemia; 4-active infections include conditions like urinary tract infection, pneumonia, and viral illnesses.

Table 1: Inclusion and exclusion criteria.

Acquisition	Analysis
Liver T2* measurement from multiecho gradient echo acquisition in an abdominal transverse plane	Measure of total body iron
Sagittal in-plane velocity-encoded cine through the descending thoracic aorta	Measure of iron stores
3D carotid time of flight scan (TOF)	Localize sections through CCA, proximal ICA and mid ICA
Carotid artery wall T2* measurement	Prescribed at 3 carotid locations on right and 3 locations on left defined from TOF
High temporal resolution cine through bilateral common carotid arteries	Carotid artery distensibility
3D noncontrast T1W-TSE carotid MRA	Vessel wall volume measurement

NOTES: CCA=common carotid artery, ICA=internal carotid artery, T1W-TSE=T1-weighted turbo spin echo, MRA=magnetic resonance angiogram

Table 2: MRI Protocol.

The multi-echo gradient echo images (Figure 1) are processed offline by drawing a region of interest (ROI) encompassing a nonvascular region of the liver for liver T2* (a well-validated noninvasive estimate of tissue iron content [9]) using semi-automated software developed in-house for carotid artery wall T2* measurement [10]. The in-plane velocity-encoded cine images (Figure 1) are processed offline using in-house software that automatically detects the time (ms after R wave) of the foot of aortic velocity upslope at each pixel in the descending aorta, then computes pulse wave velocity from a linear fit of distance vs. time-to-peak [11].

To insure reproducibility of vessel wall measurement location across serial MRI scans, each subject's T1-W TSE acquisition images are co-registered using 3D postprocessing software (FUSION Siemens Healthcare; Princeton, New Jersey).Multiplanar (MPR) images perpendicular to the arteries are generated at the same location on the co-registered data sets by one observer. Five consecutive 1 mm thickness slices are generated from each CCA and ICA, with the most cranial slice for CCA volumes located just below the carotid bulb and the most caudal slice for ICA volumes located just above the carotid bifurcation (Figure 2). Using the MPR images, two experienced observers measure lumen area and lumen plus wall areas by delineating the inner and outer border of the vessel wall. Vessel wall area is calculated by subtracting lumen area from the outer border enclosed area. Volume carotid wall for each of the four locations (right CCA and ICA, left CCA and ICA) will be calculated by multiplying the sum of the five slices wall areas with the slice thickness. A total carotid volume for a subject at a time point will be generated by summing the four wall volumes.

To calculate carotid distensibility, end systolic (As) and end diastolic (Ad) areas of the carotid lumen are measured off-line three times (Medviso AB; Lund, Sweden). All measurements for each artery are averaged and distensibility is calculated using the following formula: distensibility= [As-Ad)/As] ÷ (systolic BP – diastolic BP) in kPa^{-1}.

Statistical and Ethical Considerations

Sample size calculation

The primary outcome on which sample size is based is arterial

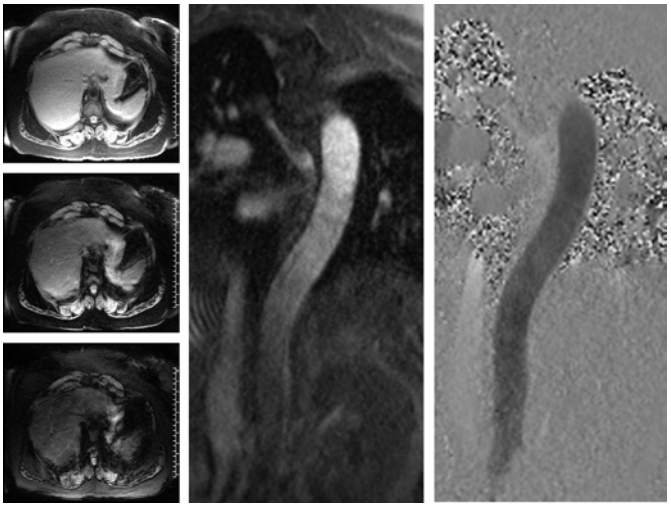

Figure 1: Left panels: Images obtained at serial echo times (top: 1.9 ms, middle: 5 ms, bottom: 8.1 ms) from a tranverse plane abdominal multiecho gradient echo acquisition show the images used for liver T2* computation, a well-validated noninvasive technique to estimate liver iron content. In the absence of secondary causes of hepatic iron overload, liver iron content may be considered a suitable surrogate for total body iron. Middle panel: magnitude image showing a longitudinal section of the descending aorta. Right panel: velocity-encoded image showing in-plane velocities in the descending aorta, from which pulse wave velocity is calculated.

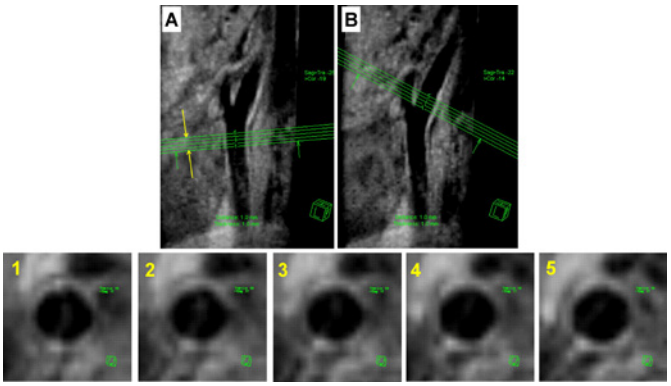

Figure 2: 3D noncontrast T1W-TSE MRI shows right (A) and left (B) carotid arteries along their lengths. Multiplanar reformatted sections for vessel wall volume are generated from the 3D acquisition over the planes shown in green; panels 1 through 5 below show representative sections for the right common carotid artery.

wall T2* measurement. Using the preliminary data from four women with CVD risk factors who underwent baseline and 1-year follow-up arterial T2* measurements, we expect that the arterial wall T2* in perimenopausal women have a mean ranging from 25 ms to 53 ms and a standard deviation of 7 ms. Assuming a conservative Bonferroni adjustment to account for the two possible pairwise comparisons (baseline vs. year 1 and year 1 vs. year 2), we used a Type I error rate of .025 (.05/2=.025). The sample size was calculated based on a paired sample *t*-test (one-sided) with a power of 80%, a correlation of 0.6 and 2.0 ms as the smallest detectable difference in arterial wall T2*. When the sample size is adjusted to account for 9% of patients unable to undergo MRI due to claustrophobia or obesity and an additional 12% of patients not completing follow-up due to various reasons (dropout, death, etc.), the required sample size is 100 for perimenopausal women with CVD risk factors. Assuming a two-sided test at alpha = 0.05 and a coefficient of variation of 88% [12], a sample size of 100 cases and 15 controls will provide 91% power to detect a two-fold difference in serum hepcidin levels at two year follow-up.

Statistical analysis

Demographic, medical history and other baseline variables will be summarized as appropriate to the type of data. Summary statistics will include the number of observations available, mean, standard deviation, median, minimum, and maximum for continuous variables such as vessel wall T2*, vessel wall volume, and carotid artery distensibility. Descriptive statistics will also be calculated for binary variables such as smoker vs. nonsmoker, diabetes and statin drug use. Cardiovascular disease (CVD) event risk score is expressed as a number of points between -2 and 21 (with values below -2 assigned to -2, and values above 21 assigned to 21), which is computed based on the following clinical variables: age, gender, systolic blood pressure, diabetes Y/N, tobacco Y/N, total cholesterol, and HDL cholesterol level [13].

To examine the decrease of arterial wall T2* in women transitioning from perimenopausal to postmenopausal status, marginal models (GEE) will be used. GEE is a flexible approach to produce robust estimates of covariate effects after adjusting for the within-person correlation in outcomes between the three clinical assessments. It is well suited to this balanced longitudinal design with three repeated clinical assessments. Analyses will be conducted in SAS by fitting linear spline models with a common knot at the time of the second clinical assessment (year 1), which is helpful to assess the potential non-linear trends in the mean arterial wall T2* over time. The regression coefficients with respect to the assessment time will be used to test whether the T2* decreases over the transition period (from baseline to year 1 and from year 1 to year 2) as hypothesized due to carotid iron increase. In the marginal models (GEE), covariates will be included as potential confounders, such as serum estradiol level, statin drug use, BMI, CVD event risk score, etc. When sample sizes permit, some interaction terms will be explored in the modeling procedure.

To assess the association between carotid artery wall T2* and wall volume or distensibility, similar marginal models (GEE) will be used with a common knot at the time of the second clinical assessment (year

Variable	Value
Race	
Caucasian	77
Black	20
Hispanic	3
Hyperlipidemia, %	86
Diabetes mellitus, %	27
Hypertension, %	81
Smoker, %	38
Age, years	49.8 ± 3.9*

*mean ± standard deviation

Table 3: Characteristics of Enrolled Participants to Date (N=100).

Variable	Value
High-sensitivity c-reactive protein, mg/dL	4.3 ± 4.3
Hematocrit, %	39.5 ± 3.5
Total cholesterol, mg/dL	204 ± 45
High-density lipoprotein, mg/dL	53.2 ± 16.2
Low-density lipoprotein, mg/dL	119.5 ± 41.8

All values are expressed as mean ± standard deviation

Table 4: Baseline Serologies of Enrolled Participants to Date (N=100).

1). In this linear spline model, the outcome measure carotid artery wall T2* will be regressed onto wall volume and distensibility by adjusting for the assessment time with a knot at year 1 and potential confounders including serum estradiol level, hsCRP, statin drug use, BMI, dietary iron intake, and CVD risk score.

Analyses will be conducted in SAS by fitting linear spline models with a common knot at the time of the second clinical assessment (year 1), which is helpful to assess the potential non-linear trends in the mean plasma hepcidin level over time. The regression coefficients with respect to the assessment time will be used to test whether the outcomes increase over the transition period (from baseline to year 1 and from year 1 to year 2) as hypothesized. In the marginal models, covariates will be included as potential confounders, such as serum estradiol level, statin drug use, BMI, CVD event risk score, etc. When sample sizes permit, some interaction terms will be explored in the modeling procedure. For the marginal models, the normality assumption for the plasma hepcidin level will be assessed to determine whether a certain transformation of the outcome is needed. Our power analysis for detecting yearly differences in plasma hepcidin (from baseline to year 1 and from year 1 to year 2) indicates that we have a power of more than 93.9% to detect a true difference of 0.4 nM in plasma hepcidin using the above sample size.

We will also extend our marginal models for serum hepcidin level to include the control data. The extended models will include effects for group (case or control) and group-by-time interactions to allow the linear splines to differ by case/control status. Our primary analysis will be a comparison of serum hepcidin level between cases and controls at two year follow-up. As a secondary analysis, we will test for differences in the linear splines between cases and controls to determine if differences between the groups change over time (i.e., a test of time-by-group interaction). A similar approach will be used to compare vessel wall T2* measurements in cases and controls.

Ethical considerations

The study is conducted according to the principles of the Declaration of Helsinki. The study design, all research aims and the specific measurements in this trial have been approved by the Institutional Review Board, and only participants who provide written informed consent after sufficient time to review study information undergo study procedures.

Data management and privacy protection

Data are manually entered into an electronic database by study investigators and research staff from written case report forms and manually-processed with periodic audits by research staff to insure quality of manual data entry. Study data are analyzed using unique subject identifiers that do not enable identification of individual subjects.

Results

While the primary focus of this work is to provide the design and rationale of our prospective clinical study, we have made considerable progress in enrollment to date. The characteristics of study participants are summarized in Table 3. Claustrophobia precluded completion of baseline evalution in 5 subjects. Data analysis is ongoing as the study hypotheses are based on changes over 2 years in serologies and imaging parameters. Description of baseline serologic studies in the cohort enrolled to date is provided in Table 4.

Discussion

The present study for the first time evaluates longitudinal changes in the arterial wall across the menopause transition that may be related to the cessation of monthly iron loss and may help explain the increased risk of atherosclerotic events seen in post- vs. pre-menopausal women. Having validated vessel wall T2* measurement as a reproducible, noninvasive map of arterial wall iron allows us to generate this evidence using serial evaluation of perimenopausal women at high risk of developing atherosclerosis. Arterial wall iron quantification with vessel wall volume and physiologic measures including carotid artery distensibility and aortic pulse wave velocity may reveal vascular abnormalities that precede clinically-evident atherosclerotic plaque.

Araujo et al. [14] showed that iron overload augments atheroma formation in hypercholesterolemic rabbits. Iron aggregates were seen in the arterial intima of the iron-overloaded rabbits suggesting that iron overload augments the formation of atherosclerotic lesions. In autopsy-derived coronary arteries and thoracic aortas, Yuan [15] found pronounced ferritin accumulation, intra-macrophage low-molecular-weight iron and macrophage-derived foam cells in atherosclerotic lesions; normal arterial tissues lacked CD68 (macrophage identifier) and ferritin positivity. Yet for all of the mechanistic appeal of iron as a contributor to atherosclerosis, many studies of epidemiology, genetics and therapeutics to lower serum iron levels have been largely negative. Danesh et al. published a meta-analysis in 1999 looking at serum levels of ferritin, tranferrin saturation, total iron binding capacity and iron and found no predictive value of coronary heart disease risk [16]. Studies in patients with hemochromatosis have notably found *less* atherosclerosis in patients with genetically-induced increases in total body iron [6,17]. Studies using phlebotomy or blood donation to lower cardiovascular events have found that these methods lowered serum iron but did not affect cardiovascular events [18,19].

Our study design includes assessment of hepcidin, a circulating peptide and central regulator of iron metabolism that controls iron uptake and release by macrophages. Thus, studying changes in hepcidin levels in parallel with vessel wall measurements allows direct investigation of atherosclerosis substrate after monthly iron loss ceases. High hepcidin levels have been reported in patients with inflammation and certain anemias who have increased macrophage iron [26,27]. This may explain why epidemiologic studies ignoring the role of hepcidin have provided inconsistent results [16].

Thus, hepcidin represents a potentially important yet unexplored link between inflammation, a well-established risk factor of cardiovascular disease, and iron homeostasis. Missing from prior studies of iron and atherosclerosis risk to date have been (1) direct iron measurements in arterial wall in humans to corroborate the positive results of animal studies and (2) any consideration of hepcidin, without which iron cannot enter macrophages. By incorporating these 2 crucial components, our work may overcome the pitfalls that have plagued prior studies that have been unable to provide conclusive evidence relating iron and atherosclerosis.

Conclusion

The current trial is the first longitudinal study of perimenopausal changes with suitable clinical, serologic and imaging endpoints to measure the extent to which vascular changes that precede atherosclerosis development may be attributable to cessation of

monthly iron loss. By using *in vivo* vessel wall iron measurement, we may identify novel mechanisms by which the gap in incident CVD between women and men rapidly closes after menopause. If arterial wall iron is shown to increase in women after menopause, we will have identified a truly novel target for prevention where current approaches directed solely at hormonal changes have fallen short in delivering meaningful cardiovascular risk reduction.

Acknowledgements

This study was funded by NIH R01 HL095563.

References

1. Kannel WB, Wilson PW (1995). Risk factors that attenuate the female coronary disease advantage. Arch Intern Med 155: 57-61.
2. Brass LM (2004) Hormone replacement therapy and stroke. Clinical trials review 35: 2644-2647.
3. Rossouw JE, Anderson GL, Prentice RL, LaCroix AZ, Kooperberg C, et al. (2002) Risks and benefits of estrogen plus progestin in healthy postmenopausal women: principal results from the Women's Health Initiative randomized controlled trial. JAMA 288: 321-333.
4. Hulley S, Grady D, Bush T, Furberg C, Herrington D, et al. (1998) Randomized trial of estrogen plus progestin for secondary prevention of coronary heart disease in postmenopausal women. Heart and Estrogen/progestin Replacement Study (HERS) Research Group. JAMA 280: 605-613.
5. Sullivan JL (1981) Iron and the sex difference in heart disease risk. Lancet 13: 1293-1294.
6. Ellervik C, Birgens H, Tybjaerg-Hansen A, Nordestgaard BG (2007) Hemochromatosis genotypes and risk of 31 disease endpoints: meta-analyses including 66,000 cases and 226,000 controls. Hepatology 46: 1071-1080.
7. Song Y, Manson JE, Buring JE, Liu S (2004) A Prospective study of red meat consumption and type 2 diabetes in middle-aged and elderly women. Diabetes Care 27: 2108-2115.
8. Lee JS, LaCroix AZ, Wu L, Cauley JA, Jackson RD, et al. (2008) Associations of serum sex hormone-binding globulin and sex hormone concentrations with hip fracture risk in postmenopausal women. J Clin Endocrinol Metab 93: 1796-1803.
9. Anderson LJ, Holden S, Davis B, Prescott E, Charrier CC, et al. (2001) Cardiovascular T2-star (T2*) magnetic resonance for the early diagnosis of myocardial iron overload. European Heart Journal 22: 2171-2179.
10. Sharkey-Toppen T, Clymer BD, Maiseyeu A, Tran T, Mihai G, et al. (2010) Improved T2* estimation technique in human carotid arteries. Proceedings of the International Society for Magnetic Resonance in Medicine 18th Scientific Meeting.
11. Giri SS, Ding Y, Nishijima Y, Pedraza-Toscano A, Burns PM, et al. (2007) Automated and accurate measurement of aortic pulse wave velocity using magnetic resonance imaging. Computers in Cardiology 34: 661-664.
12. Murphy AT, Witcher DR, Luan P, Wroblewski VJ. (2007) Quantitation of hepcidin from human and mouse serum using liquid chromatography tandem mass spectrometry. Blood 110 :1048-1054.
13. D'Agostino RB Sr, Vasan RS, Pencina MJ, Wolf PA, Cobain M, et al. (2008) General cardiovascular risk profile for use in primary care: the Framingham Heart Study. Circulation 117: 743-753.
14. Araujo JA, Romano EL, Brito BE, Parthe V, Romano M, et al (1995). Iron overload augments the development of atherosclerotic lesions in rabbits. Arterioscler Thromb Vasc Biol 15: 1172-1180.
15. Yuan XM (1999) Apoptotic macrophage-derived foam cells of human atheromas are rich in iron and ferritin, suggesting iron-catalysed reactions to be involved in apoptosis. Free Radic Res 30: 221-231.
16. Danesh J, Appleby P (1999) Coronary heart disease and iron status: meta-analyses of prospective studies. Circulation 99: 852-854.
17. Miller MM, Hutchins, GM (1994) Hemochromatosis, multiorgan hemosiderosis, and coronary artery disease. JAMA 272: 231-233.
18. Ascherio A, Rimm EB, Giovannucci E, Willett WC, Stampfer MJ (2001) Blood donations and risk of coronary heart disease in men. Circulation 103: 52-57.
19. Zacharski LR, Chow BK, Howes PS, Shamayeva G, Baron JA, et al. (2007) Reduction of iron stores and cardiovascular outcomes in patients with peripheral arterial disease: a randomized controlled trial. JAMA 297: 603-610.
20. Nemeth E, Rivera S, Gabayan V, Keller C, Taudorf S, et al. (2004) IL-6 mediates hypoferremia of inflammation by inducing the synthesis of the iron regulatory hormone hepcidin. J Clin Invest 113: 1271-1276.
21. Kemna E, Pickkers P, Nemeth E, van der Hoeven H, Swinkels D (2005) Time-course analysis of hepcidin, serum iron, and plasma cytokine levels in humans injected with LPS. Blood 106: 1864-1866.
22. Pak M, Lopez MA, Gabayan V, Ganz T, Rivera S (2006) Suppression of hepcidin during anemia requires erythropoietic activity. Blood 108: 3730-3735.
23. Babitt JL, Huang FW, Wrighting DM, Xia Y, Sidis Y, et al. (2006) Bone morphogenetic protein signaling by hemojuvelin regulates hepcidin expression. Nat Genet 38: 531-539.
24. Swinkels DW, Janssen MC, Bergmans J, Marx JJ (2006) Hereditary hemochromatosis: genetic complexity and new diagnostic approaches. Clin Chem 52: 950-968.
25. van Tits LJ, Jacobs EM, Swinkels DW, Lemmers HL, van der Vleuten GM, et al. (2006) Serum non-transferrin-bound iron and low-density lipoprotein oxidation in heterozygous hemochromatosis. Biochem Biophys Res Commun 345: 371-376.
26. Sullivan JL (2007) Macrophage iron, hepcidin, and atherosclerotic plaque stability. Exp Biol Med 232: 1014-1020.
27. Malyszko J, Mysliwiec M (2007) Hepcidin in anemia and inflammation in chronic kidney disease. Kidney Blood Press Res 30: 15-30.